Combined MV-LV Power Grid Operation

Combined MV-LV Power Grid Operation: Comparing Sequential, Integrated, and Decentralized Control Architectures

Sen Zhan, Johan Morren, Wouter van den Akker, Anne van der Molen, Nikolaos G. Paterakis, J. G. Slootweg
Electrical Energy Systems, Eindhoven University of Technology
Eindhoven, The Netherlands
Emails: {s.zhan, j.morren, w.f.v.d.akker, a.e.v.d.molen, n.paterakis, j.g.slootweg}@tue.nl

***Abstract*—The increasing connection of distributed energy resources (DERs) to low-voltage (LV) power grids challenges the operation of both connected LV grids and upstream medium-voltage (MV) grids, through power flow via the MV/LV transformers. Handling the coupling between MV and LV grids calls for combined MV-LV network operation models. This study develops various optimization-based models, built respectively on sequential, integrated, and decentralized control architectures. A new objective function is also designed to attain fairer DER curtailment strategies. For the decentralized architecture, this study explores the generalized Benders decomposition (GBD) and two augmented Lagrangian relaxation (ALR)-based approaches: the alternating direction method of multipliers (ADMM) and the auxiliary problem principle (APP). Computational results based on open-source Simbench networks show reduced power curtailment from the integrated architecture compared to the sequential one. For decentralization, GBD already shows superior convergence performance compared to ADMM and APP under moderate accuracy requirements. Under higher accuracy requirements, GBD maintains fast convergence, while ADMM and APP fail to converge in a reasonable number of iterations.**

***Index Terms*—Distribution system management, integrated MV-LV network operation, decentralized optimization**

I. Introduction

The increasing penetration of distributed energy resources (DERs) such as photovoltaics (PVs) to low-voltage (LV) power grids not only challenges the safety of LV grids, causing voltage issues and asset congestion but also that of upstream medium-voltage (MV) grids, through power flow via the MV-LV transformers. Widely in the literature, the operation of MV and LV grids has been separately optimized without considering their mutual impact. However, as MV and downstream LV grids are managed by the same distribution system operators (DSOs), the combined operation optimization of MV and LV grids is possible. Based on different communication structures between MV and LV grids, this study develops and compares three control architectures, including a) **sequential**: MV and LV grids are separately optimized with one iteration of information exchange on boundary variables; b) **integrated**: MV and LV grids are simultaneously optimized in a central platform; c) **decentralized**: MV and LV grids are separately optimized with multiple iterations of information exchange.

This project is funded by TKI Energie from the 'Toeslag voor Topconsortia voor Kennis en Innovatie (TKI)' from the ministry of Economical Affairs and Climate, under reference 1821401.

Few studies in the literature have considered the combined operation of MV and LV grids. In [1], the authors proposed dynamic import/export limits for prosumers to ensure network constraints are satisfied. In [2], advanced conservation voltage reduction schemes were discussed. In [3], different fair PV curtailment schemes were studied. These studies [1]–[3] are all built on the integrated architecture. There is a lack of discussion and comparison of different control architectures in the literature. For example, it is not clear how much benefit the integrated architecture can bring to DSOs and end-users compared to the sequential one.

Moreover, managing all DERs on a central unit can be computationally challenging and unreliable, especially when dealing with large grids. Privacy concerns can also arise. Decentralized approaches tend to better tackle large-scale problems. However, this needs to be further investigated in the context. To achieve decentralized optimization, the alternating direction method of multiplier (ADMM) has been adopted in [4] to determine PV setpoints for combined MV-LV networks. The generalized Benders decomposition (GBD) has also been applied under the context of integrated transmission-distribution grids [5], and integrated electricity-gas systems [6]. However, there is a lack of empirical comparison between the ALR and GBD approaches in the literature. As pointed out in [7], numerical simulations are key for understanding their practical performance. Such comparison between ALR and the KKT-based decentralized approaches for the DC-OPF problem was, nevertheless, made in [8].

Concerning the objective function design for distribution system management, minimizing power losses and minimizing generation curtailment are commonly seen in the literature. As generation curtailment in LV grids is generally not financially compensated, fairness among end-users with different generation capacities is also an important consideration. Although the proposed PV curtailment schemes in [3] lead to improved fairness, a large increase in PV curtailment is seen in their case study. The authors in [9] presented a logarithmic objective function for improved fairness, which however requires a

978-1-6654-0557-7/22/$31.00 ©2022 IEEE

piecewise-linear approximation for implementation in modern solvers. This study proposes a simple yet effective quadratic objective function design that considers both minimizing generation curtailment and improving fairness. As seen in [3], fairness for PV curtailment can be defined in different ways. This study focuses on the proportional fairness which requires all generation units to have similar curtailment ratios with respect to their forecasted generation.

To summarize, this paper focuses on the combined MV-LV network operation, making contributions to the objective function design, comparing control architectures, and simulating the practical performance of algorithms for implementing the decentralized architecture. Specifically:

- This study compares three different control architectures for the combined MV-LV network optimization. The discussion and comparison of architectures for combined MV-LV network operation are missing in the literature. The benefit of the integrated architecture compared to the sequential one is quantified in a case study. This facilitates DSOs to employ a suitable architecture when considering the combined MV-LV network operation.
- To address the lack of empirical comparison between different decentralization approaches, numerical tests are conducted for two ALR-based approaches (ADMM and APP) and GBD for implementing the decentralized architecture, which is key for understanding their practical performance and applicability.
- A simple yet effective quadratic objective function is proposed which combines the ideas of minimized generation curtailment and improved fairness.

The remainder of this paper is organized as follows: Section II presents a mathematical model for distribution network modeling and the new objective function design. Section III elaborates on the three control architectures and the decentralized operation strategies based on GBD, ADMM, and APP, respectively. A case study and simulation results are reported in Section IV. Section V concludes this study.

II. Integrated MV-LV Network Modeling

A. Distribution Network Modeling

An integrated MV-LV network operation model is presented in this section. To represent power flow relations, the linearized branch flow model [10] is adopted for both MV and LV networks, which is built on the assumption that branch losses are negligible compared to branch power flow. For the investigated distribution networks, branch losses account for on average around 0.5% of branch power flow, which leads to highly accurate results for the developed model. The model is formulated as (1). Notations are provided in Table I.

TABLE I
Notation for optimization model.

Notation	Physical meaning	Unit
$\mathcal{N}, \mathcal{E}, \mathcal{T}$	Collections of nodes, cables, transformers	-
Parameters		
$\tilde{p}_j^g$	Forecasted power generation for node j	MW
p_j^d, q_j^d	Active/reactive power demand for node j	MW
r_{ij}, x_{ij}	Resistance/reactance between node i and j	Ω
$v_j^{min/max}$	Min/max voltage magnitude squared of node j	$(kV)^2$
S_{ij}^{max}	Max apparent power between node i and j	MVA
S_j^g	Generation unit capacity at node j	MVA
ϕ	Maximum phase angle	rad
τ	Transformer turns ratio	-
Variables		
p_j^g, q_j^g	Active/reactive power generation for node j	MW
Dependent		
P_{ij}, Q_{ij}	Active/reactive power flow from node i to j	MW
v_j	Voltage magnitude squared of node j	$(kV)^2$

$$p_j^g - p_j^d = \sum_{k:j\to k} P_{jk} - \sum_{i:i\to j} P_{ij}, \forall j \in \mathcal{N} \tag{1a}$$

$$q_j^g - q_j^d = \sum_{k:j\to k} Q_{jk} - \sum_{i:i\to j} Q_{ij}, \forall j \in \mathcal{N} \tag{1b}$$

$$v_j = v_i - 2\left(r_{ij}P_{ij} + x_{ij}Q_{ij}\right), \forall (i,j) \in \mathcal{E} \tag{1c}$$

$$v_j = \tau^2 v_i - 2\left(r_{ij}P_{ij} + x_{ij}Q_{ij}\right), \forall (i,j) \in \mathcal{T} \tag{1d}$$

$$P_{ij}^2 + Q_{ij}^2 \le (S_{ij}^{max})^2, \forall (i,j) \in \mathcal{E} \cup \mathcal{T} \tag{1e}$$

$$v_j^{min} \le v_j \le v_j^{max}, \forall j \in \mathcal{N} \tag{1f}$$

$$p_j^g \le \tilde{p}_j^g, \forall j \in \mathcal{N} \tag{1g}$$

$$(p_j^g)^2 + (q_j^g)^2 \le (S_j^g)^2, \forall j \in \mathcal{N} \tag{1h}$$

$$-\tan_\phi p_j^g \le q_j^g \le \tan_\phi p_j^g, \forall j \in \mathcal{N} \tag{1i}$$

Constraints (1a)-(1b) represent active and reactive power balance for all nodes. Constraints (1c)-(1d) dictate the voltage relation across cables and transformers. Grid limits are enforced in (1e)-(1f), pertaining to thermal limits of grid assets and statutory voltage limits respectively. Constraints (1g)-(1i) concern individual generators, enforcing, respectively, power, capacity, and power factor limits.

B. Objective Function Design

For distribution system management, the objective function can take various forms, such as minimizing losses. This study focuses on minimizing generation curtailment to minimize the impact on end-users while keeping grid safety. A straightforward implementation is through (2a), which minimizes total curtailment throughout the grid. However, such formulation can result in unfair power curtailment, as validated in Section IV, penalizing largely end-users located at the end of distribution feeders. Moreover, with the linear objective function, the optimal solution can be non-unique, which may raise additional issues when implementing such control decisions.

$$\underset{p_j^g, q_j^g, \forall j\in\mathcal{N}}{\text{minimize}} \sum_{j\in\mathcal{N}} (\tilde{p}_j^g - p_j^g) \tag{2a}$$

$$\underset{p_j^g, q_j^g, \forall j\in\mathcal{N}}{\text{minimize}} \sum_{j\in\mathcal{N}} \left[(\tilde{p}_j^g - p_j^g)^2 / \tilde{p}_j^g\right] \tag{2b}$$

In this regard, a simple yet effective quadratic objective function (2b) is proposed to improve the proportional fairness

in this study. The reasoning behind this formulation is that for generators with higher curtailment percentages, the marginal costs for curtailing additional power are higher. For generators with the same curtailment percentage, the marginal costs for curtailing additional power are the same, thus pushing all generators to a similar curtailment percentage. This is demonstrated through the first-order derivative in (3). While for the linear objective function, the marginal costs are the same for generators with different curtailment percentages, which are derived from its constant derivative. This objective function is thus not able to penalize generators with lower curtailment percentages. Besides the fairness consideration, with the quadratic hence strongly convex objective function, a unique optimal solution is admitted for the model.

$$\frac{d\left[(\tilde{p}_j^g - p_j^g)^2/\tilde{p}_j^g\right]}{\underbrace{-dp_j^g}_{\text{Minus for power curtailment}}} = 2 \underbrace{(\tilde{p}_j^g - p_j^g)/\tilde{p}_j^g}_{\text{Curtailment percentage}} \tag{3}$$

III. Control Architectures

A. Overview of Control Architectures

To consider the coupling between MV and LV grids, this study develops and compares three control architectures for the combined MV-LV system management. Table II summarizes their characteristics. To simplify the formulation, the optimization model is re-written in a compact form as (4), where (x, z) are decision variables for the MV grid, (y_i, w_i) are decision variables for the LV grid indexed i. The variables are distinguished such that $z = [z_1, z_2, ...]$ and w_i are respectively boundary variables for the MV grid and LV grids, which are variables shared by MV and LV grids at the connection points between them. $f(\cdot)$ and $g_i(\cdot)$ are their respective objective functions, while Ω and Ψ_i are their respective feasible regions. The corresponding dual variables are represented as λ_i. The last constraint, which couples the MV and LV grids, represents the duplicated boundary variables at the MV side of the MV-LV transformers, such that $z_i = w_i = [P_i, Q_i, v_i]$, denoting respectively, active power flow, reactive power flow, and squared voltage magnitude.

$$\begin{aligned} \underset{x,z,y_i,w_i}{\text{minimize}} \quad & f(x,z) + \textstyle\sum_i g_i(y_i, w_i) \\ \text{subject to} \quad & (x,z) \in \Omega \\ & (y_i, w_i) \in \Psi_i, \forall i \\ & z_i = w_i : \lambda_i, \forall i \end{aligned} \tag{4}$$

1) Integrated: The integrated architecture is a direct implementation of the model (4), in which the topology of the integrated grid and generation/load profiles are collected in a central unit. The model (4) is formulated and handled by a solver. The optimized control decisions are then dispatched to individual generators. Due to the convexity of the model (4), this can generally achieve a globally optimal solution.

2) Sequential: The sequential architecture represents a hierarchical optimization scheme, in which the MV grid first takes LV grids as lumped nodes using aggregated generation/load profiles and an aggregated generation capacity and runs its optimization model. Following this, the boundary variables z_i are dispatched to individual LV grids. The LV grids then manage their assets to follow the boundary variables as closely as possible while minimizing their costs. This is implemented by augmenting the LV grids' objective functions with extra penalty terms $\rho\|w_i - z_i\|^2$ penalizing the difference between the dispatched boundary variables z_i and their own decisions on boundary variables w_i, where ρ is a large positive parameter. When the LV grids accurately follow the dispatched boundary variables, i.e. $w_i = z_i$, this procedure gives a feasible but usually non-optimal solution to (4).

TABLE II
Comparison of integrated, sequential, and decentralized architectures.

Architectures	Integrated	Sequential	Decentralized
Optimality	Yes	No	Yes
Decentralized	No	Yes	Yes
Communication	1 iteration	1 iteration	multiple iterations
Computation	Fast (small scale), slow (large scale)	Very Fast	Fast (large scale), slow (small scale)

3) Decentralized: The decentralized architecture is built on the observation that the MV grid and LV grids are weakly coupled, through the MV-LV transformers, modeled as the duplicated boundary variables. In the following sections, two augmented Lagrangian relaxation-based schemes and the generalized Benders decomposition approach are developed for the decentralized implementation of the problem (4). Due to convexity and strong duality (from the weak Slater's condition) of the problem (4), these decentralized schemes generally converge to the globally optimal solution, thus achieving the same results as the integrated architecture. Their scalability to tackle large-scale instances has also been demonstrated in different case studies [11], [12]. Detailed implementation of these decentralization approaches is presented below.

B. Augmented Lagrangian Relaxation

$$\begin{aligned} \underset{\lambda_i}{\text{maximize}} \Bigg\{ & \underset{(x,z)\in\Omega,(y_i,w_i)\in\Psi_i}{\text{minimize}} f(x,z) + \sum_i g_i(y_i,w_i) \\ & + \sum_i \lambda_i(z_i - w_i) + \underbrace{\sum_i \frac{1}{2}\rho_i\|z_i - w_i\|^2}_{\text{Augmented term}} \Bigg\} \end{aligned} \tag{5}$$

The augmented Lagrangian relaxation is based on the Lagrangian relaxation, but deals with an extra quadratic penalty term for better convergence properties [11]. This is equivalent to adding the augmented term in the objective function of (4), which does not change its solution, due to the last constraint. The dual problem of (4) is given in (5), with the extra augmented term. Without the augmented term, when fixing λ_i, the inner minimization problem can be solved separately for the MV and LV grids. With the subgradient method to update λ_i, this forms the foundation of the dual decomposition. ADMM and APP are two approaches to handle the augmented term and to make the inner minimization problem again

Algorithm 1: Implementation of ADMM and APP

Initialize: $\lambda_i^{(1)}, \rho_i^{(1)}, w_i^{(0)}, z_i^{(0)}, k \leftarrow 0$, primal residual $r_i^{(0)}$, dual residual $s_i^{(0)}$, $\mu \leftarrow 10$, $\tau \leftarrow 2$, tolerance $\epsilon \leftarrow 10^{-4}/10^{-6}$, $k^{max} \leftarrow 1000$

while $\left(\min(\|r_i^{(k)}\|, \|s_i^{(k)}\|) > \epsilon$ **and** $k < k^{max}\right)$ **do**
  $k \leftarrow k+1$;
  if *ADMM* **then**
    $x^{(k)}, z^{(k)} \leftarrow \underset{(x,z)\in\Omega}{\text{argmin}}\ f(x,z) + \sum_i \lambda_i^{(k)} z_i + \sum_i \frac{1}{2}\rho_i^{(k)} \|z_i - w_i^{(k-1)}\|^2$;
    $y_i^{(k)}, w_i^{(k)} \leftarrow \underset{(y_i,w_i)\in\Psi_i}{\text{argmin}}\ g_i(y_i,w_i) - \lambda_i^{(k)} w_i + \frac{1}{2}\rho_i^{(k)} \|z_i^{(k)} - w_i\|^2$;
  else if *APP* **then**
    $x^{(k)}, z^{(k)} \leftarrow \underset{(x,z)\in\Omega}{\text{argmin}}\ f(x,z) + \sum_i \lambda_i^{(k)} z_i + \sum_i \rho_i^{(k)} (z_i^{(k-1)} - w_i^{(k-1)}) z_i + \sum_i \rho_i^{(k)} \|z_i - z_i^{(k-1)}\|^2$;
    $y_i^{(k)}, w_i^{(k)} \leftarrow \underset{(y_i,w_i)\in\Psi_i}{\text{argmin}}\ g_i(y_i,w_i) - \lambda_i^{(k)} w_i - \sum_i \rho_i^{(k)} (z_i^{(k-1)} - w_i^{(k-1)}) w_i + \sum_i \rho_i^{(k)} \|w_i - w_i^{(k-1)}\|^2$;
  end
  $r_i^{(k)} \leftarrow z_i^{(k)} - w_i^{(k)}, s_i^{(k)} \leftarrow \rho_i^{(k)} (w_i^{(k)} - w_i^{(k-1)})$;
  $\lambda_i^{(k+1)} \leftarrow \lambda_i^{(k)} + \rho_i^{(k)} (z_i^{(k)} - w_i^{(k)})$;
  if $\|r_i^{(k)}\| > \mu \|s_i^{(k)}\|$ **then** $\rho_i^{(k+1)} \leftarrow \tau \rho_i^{(k)}$;
  else if $\|s_i^{(k)}\| > \mu \|r_i^{(k)}\|$ **then** $\rho_i^{(k+1)} \leftarrow \rho_i^{(k)} / \tau$;
  else $\rho_i^{(k+1)} \leftarrow \rho_i^{(k)}$;
end

Algorithm 2: Implementation of GBD

Initialize: $k \leftarrow 0$, lower bound LB, upper bound UB, tolerance $\epsilon \leftarrow 10^{-4}/10^{-6}$, $k^{max} \leftarrow 1000$

while $\left(UB - LB > \epsilon$ **and** $k < k^{max}\right)$ **do**
  $k \leftarrow k+1$;
  $x^{(k)}, z^{(k)}, LBD_i^{(k)} \leftarrow \left\{ \underset{(x,z)\in\Omega}{\text{argmin}}\ f(x,z) + \sum_i LBD_i \text{ s. t. optimality cuts; feasibility cuts} \right\}$; `/* Master problem */`
  $LB \leftarrow f(x^{(k)}, z^{(k)}) + \sum_i LBD_i^{(k)}$;
  Solve $\left\{ \underset{(y_i,w_i)\in\Psi_i}{\text{minimize}}\ g_i(y_i,w_i) \text{ s. t. } w_i \le z_i^{(k)} : \lambda_i \right\}$; `/* Subproblems */`
  if *optimal* **then**
    Acquire primal/dual solution: $y_i^{(k)}, w_i^{(k)}, \lambda_i^{(k)}$;
    Add an optimality cut to master probelm: $LBD_i \ge g_i(y_i^{(k)}, w_i^{(k)}) + (\lambda_i^{(k)})^T (w_i^{(k)} - z_i)$
  else if *infeasible* **then**
    Solve $\left\{ \underset{(y_i,w_i)\in\Psi_i}{\text{minimize}}\ \alpha \text{ s. t. } w_i \le z_i^{(k)} + \alpha \mathbf{1} : \lambda_i \right\}$;
    Acquire primal/dual solution: $w_i^{(k)}, \lambda_i^{(k)}$;
    Add a feasibility cut to master problem: $(\lambda_i^{(k)})^T (w_i^{(k)} - z_i) \le 0$
  end
  if *All subproblems are optimal* **then**
    $UB \leftarrow f(x^{(k)}, z^{(k)}) + \sum_i g_i(y_i^{(k)}, w_i^{(k)})$
  end
end

separable. ADMM is based on updating boundary variables in an alternating fashion, while APP linearizes the augmented term at the current iterate and adds quadratic separable terms. Detailed implementation of ADMM and APP is shown in Algorithm 1, covering steps of primary variable update, primal and dual residual calculation, dual variable update, and penalty parameter update which follows the practice in [11].

C. Generalized Benders Decomposition

The generalized Benders decomposition is a generalization of the classic Benders decomposition to support handling nonlinear subproblems [13]. The approach applies to an optimization problem in the case when fixing some variables, also known as the complicating variables, the problem can be solved separately. In this study, when fixing the boundary variables at the MV/LV interfaces, the LV grids can be separately optimized. The essence of GBD is projecting the subproblems on the boundary variables z_i, deriving $v_i(z_i)$ and $\Omega(z_i)$, which are respectively, the optimal value of the i-th subproblem's objective function as a function of the boundary variables, and the set of boundary variables such that the subproblems are feasible. Explicit expressions of $v_i(z_i)$ and $\Omega(z_i)$ are generally not available. GBD handles this by systematically deriving a series of affine cuts, known as the optimality cuts and the feasibility cuts, shown in Fig. 1. With more such cuts, $v_i(z_i)$ and $\Omega(z_i)$ are better approximated, eventually allowing us to derive an accurate solution. The implementation process is elaborated in Algorithm 2. Reference [13] elaborates on the idea of projection and provides the formal derivation of optimality and feasibility cuts.

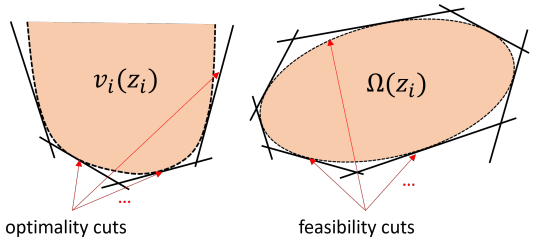

Fig. 1. Benders decomposition: using optimality cuts and feasibility cuts to approximate objective function and feasible region.

IV. Case Study

A. Case Description

To evaluate the proposed objective function, compare different control architectures and investigate the practical per-

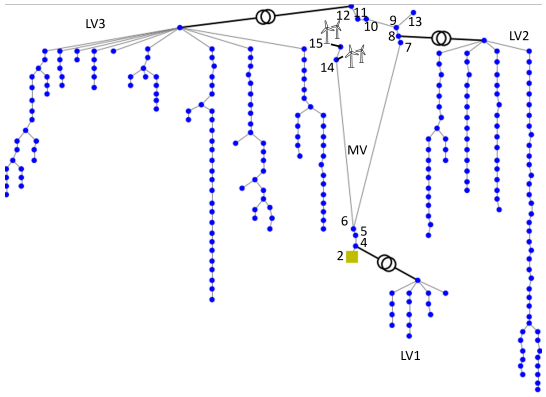

Fig. 2. Test network topology: 3 LV networks connected to a MV feeder.

TABLE III
COMPARISON BETWEEN LINEAR, LOGARITHMIC, AND QUADRATIC OBJECTIVE FUNCTIONS. RESULTS AVERAGED FOR THE 22 TIME STEPS.

Objective	Total curtail. (kWh)	Mean curt. ratio (%)	Std. dev. (%)	Compute. time (s)
Linear	2819.7	26.3	36.7	5.1
Logarithmic [9]	2819.8	19.2	10.8	5.5
Quadratic	2820.3	19.2	10.4	5.1

formance of different decentralization approaches, a case study based on the open-source Simbench project data [14] is conducted. Fig. 2 shows the network topology, which is constructed with one MV rural network feeder (13 nodes) and three LV rural networks (14, 96, and 128 nodes respectively). Considered distributed generators include two wind farms (1.7 and 4 MW respectively) in the MV network and rich PVs in LV networks. For easier comparison between different control architectures, this study focuses on addressing overvoltage and congestion problems from distributed generators through curtailing their power generation and reactive power compensation from themselves. Time series load and generation profiles are also available in the Simbench project. The following modifications are made to the test network: 1) The PV penetration level for LV2 and LV3 is scaled up to 80%; 2) The PV capacities for LV3 are doubled; 3) For nodes 8-13 in the MV feeder, the total PV capacity is also doubled; 4) The transformer capacities for LV2/LV3 are increased to 630 kVA. These modifications are made to simulate a futuristic high PV penetration scenario, which can easily result in grid congestion problems. Simulation results are reported as follows. The data and code are available on a Github repository [15].

B. Simulation Results

1) Objective Function Design: The quadratic objective function design is tested on the integrated architecture to solve congestion and voltage problems occurring in the simulated grid, along with the linear and the logarithmic one developed in [9]. Fig. 3 shows the distribution of generation curtailment ratios among end-users for 22 time steps when grid congestion occurs. The quadratic objective function design shows considerable improvement in the proportional fairness compared to

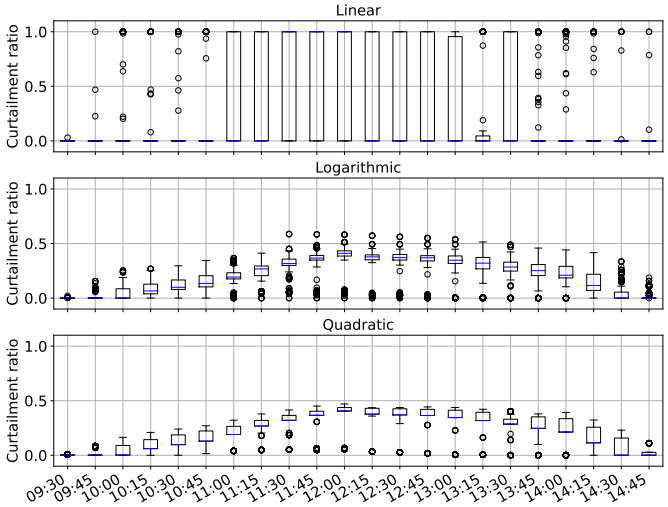

Fig. 3. Distribution of generation curtailment ratios among end-users for linear, logarithmic, and quadratic objective functions.

TABLE IV
COMPARISON BETWEEN SEQUENTIAL AND INTEGRATED ARCHITECTURES.

	Integrated	Sequential	Ratio
Total curtailment (kWh)	2820.3	2981.1	1.06
Maximum MV voltage (pu)	1.050	1.049	1.00
Maximum LV voltage (pu)	1.09	1.09	1.00
Maximum cable loading (%)	96.8	95.8	0.99
Maximum transformer loading (%)	97.7	97.8	1.00

the linear one, as seen by the smaller spread of curtailment ratios. A slight improvement is also seen compared to the logarithmic one, which is validated in Table III where the quadratic design leads to the smallest standard deviation of generation curtailment ratios. It is important to note that both the logarithmic and quadratic objectives result in negligible increases in total energy curtailment, by 0.004% and 0.02% respectively. Concerning the computational performance, the quadratic design is as fast as the linear one, while the logarithmic one takes an extra 7.8% of time due to its need for piecewise linearization. A larger network and a larger dataset are seen as necessary in future work to further compare the logarithmic and the quadratic one concerning fairness improvement and computation. Nevertheless, this case study has shown the quadratic design's satisfactory performance while retaining the advantage of a straightforward implementation.

2) Integrated & Sequential Control Architectures: This section compares the sequential and integrated control architectures. Fig. 4 shows that both the integrated and sequential architectures can fully remove the overvoltage and congestion issues occurring in the grid due to high renewable generation at all time steps. Table IV demonstrates their similar impact on the grid. However, the integrated architecture allows 5.7% less generation curtailment due to that it achieves a globally optimal solution, while the sequential architecture generally results in a feasible but non-optimal solution.

TABLE V
COMPARISON BETWEEN DIFFERENT DECENTRALIZATION APPROACHES. RESULTS AVERAGED FOR THE 22 TIME STEPS.

		Moderate accuracy: $\epsilon = 10^{-4}$			High accuracy: $\epsilon = 10^{-6}$		
Decentralization	Integrated	GBD	ADMM	APP	GBD	ADMM	APP
Curtailment (kWh)	2820.3	2823.4	2824.4	2835.5	2820.9	2823.2	2824.4
Relative error (%)	-	0.11	0.15	0.54	0.02	0.10	0.15
No. of iterations	-	16	56	124	20	566	1000
Computation (s)	5.1	37.5	75.1	166.2	44.4	649.3	1291.3

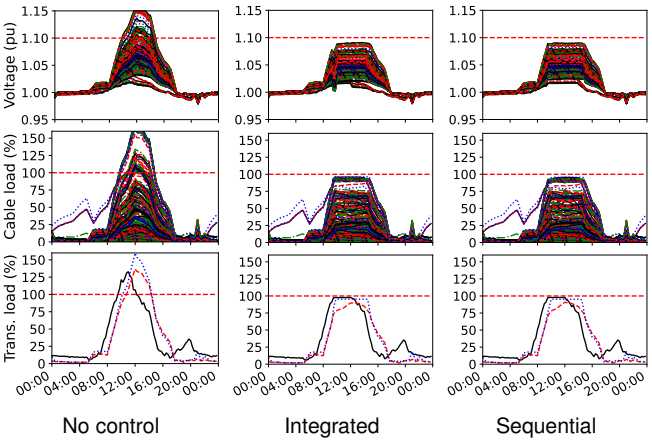

Fig. 4. Voltage, cable loading, and transformer loading throughout the simulated day. Each line corresponds to a bus, a cable, or a transformer.

3) Decentralized Optimization: The last section deals with the practical performance of different approaches applicable to building the decentralized architecture. Table V summarizes their performance under both moderate and high accuracy requirements. It is seen that all approaches generate highly accurate results, giving a maximum 0.54% error in terms of total energy curtailment. With moderate accuracy requirements, all approaches can converge, where GBD already shows faster convergence than ADMM and APP. However, with higher accuracy requirements, GBD maintains fast convergence, requiring 4 extra iterations to converge on average, while ADMM and APP fail to converge within the 1000 iteration limit in many time steps. It is also noticed that all decentralization approaches are significantly slower than the integrated architecture. However, with a larger network, a larger dataset and the exploitation of parallel computing techniques in future work, computational advantages are expected for the decentralized architecture.

V. CONCLUSIONS

This study focuses on the combined MV-LV network operation, making contributions to the objective function design, comparing control architectures, and simulating the practical performance of different approaches for implementing the decentralized architecture. Based on a case study with 1 MV feeder and 3 LV networks, it is shown that the quadratic objective function design ensures minimized while fairer generation curtailment. Comparing the sequential and integrated architectures, both can solve network issues, while the integrated architecture can reduce generation curtailment by 5.7%. For implementing the decentralized architecture, GBD already shows faster convergence with moderate accuracy requirements than ADMM and APP. With higher accuracy requirements, GBD requires a few extra iterations to converge, while ADMM and APP fail to converge in a reasonable number of iterations. It is recommended for future work to test the objective function design, control architectures, and decentralization approaches on a large network and a larger dataset to validate and generalize these findings.

REFERENCES

[1] K. Petrou, A. T. Procopiou, L. Gutierrez-Lagos *et al.*, "Ensuring Distribution Network Integrity Using Dynamic Operating Limits for Prosumers," *IEEE Trans. Smart Grid*, pp. 1–11, 2021.

[2] L. Gutierrez-Lagos and L. F. Ochoa, "OPF-Based CVR Operation in PV-Rich MV-LV Distribution Networks," *IEEE Trans. Power Syst.*, vol. 34, no. 4, pp. 2778–2789, 2019.

[3] M. Z. Liu, A. T. Procopiou, K. Petrou *et al.*, "On the Fairness of PV Curtailment Schemes in Residential Distribution Networks," *IEEE Trans. Smart Grid*, vol. 11, no. 5, pp. 4502–4512, 2020.

[4] L. Gutierrez-Lagos, M. Z. Liu, and L. F. Ochoa, "Implementable Three-Phase OPF Formulations for MV-LV Distribution Networks: MILP and MIQCP," in *2019 IEEE PES Conf. Innov. Smart Grid Technol. ISGT Lat. Am. 2019*, 2019, pp. 1–6.

[5] C. Lin, W. Wu, B. Zhang *et al.*, "Decentralized Reactive Power Optimization Method for Transmission and Distribution Networks Accommodating Large-Scale DG Integration," *IEEE Trans. Sustain. Energy*, vol. 8, no. 1, pp. 363–373, 2017.

[6] H. Gao and Z. Li, "A Benders Decomposition Based Algorithm for Steady-State Dispatch Problem in an Integrated Electricity-Gas System," *IEEE Trans. Power Syst.*, vol. 36, no. 4, pp. 3817–3820, 2021.

[7] D. K. Molzahn, F. Dörfler, H. Sandberg *et al.*, "A Survey of Distributed Optimization and Control Algorithms for Electric Power Systems," *IEEE Trans. Smart Grid*, vol. 8, no. 6, pp. 2941–2962, 2017.

[8] A. Kargarian, J. Mohammadi, J. Guo *et al.*, "Toward Distributed/Decentralized DC Optimal Power Flow Implementation in Future Electric Power Systems," *IEEE Trans. Smart Grid*, vol. 9, no. 4, pp. 2574–2594, 2018.

[9] K. Petrou, M. Z. Liu, A. T. Procopiou *et al.*, "Operating envelopes for prosumers in LV networks: A weighted proportional fairness approach," *IEEE PES Innov. Smart Grid Technol. Conf. Eur.*, pp. 579–583, 2020.

[10] M. E. Baran and F. F. Wu, "Network Reconfiguration in Distribution Systems for Loss Reduction and Load Balancing," *IEEE Trans. Power Deliv.*, vol. 4, no. 2, pp. 1401–1407, 1989.

[11] S. Boyd, N. Parikh, E. Chu *et al.*, "Distributed optimization and statistical learning via the alternating direction method of multipliers," *Found. Trends Mach. Learn.*, vol. 3, no. 1, 2010.

[12] R. Rahmaniani, T. G. Crainic, M. Gendreau *et al.*, "The Benders decomposition algorithm: A literature review," *Eur. J. Oper. Res.*, vol. 259, no. 3, pp. 801–817, 2017.

[13] A. M. Geoffrion, "Generalized Benders Decomposition," *J. Optim. Theory Appl.*, vol. 10, no. 4, pp. 237–260, 1972.

[14] S. Meinecke, D. Sarajlić, S. R. Drauz *et al.*, "Simbench—a benchmark dataset of electric power systems to compare innovative solutions based on power flow analysis," *Energies*, vol. 13, no. 12, p. 3290, Jun. 2020.

[15] S. Zhan, "Combined-MV-3LV," *GitHub repository*, 2022. [Online]. Available: https://github.com/senzhanopt/Combined-MV-3LV